

# Type-II see-saw: searching the LHC elusive low-mass triplet-like Higgses at $e^-e^+$ colliders

Saiyad Ashanujjaman<sup>1,2,\*</sup>, Kirtiman Ghosh<sup>1,2,†</sup> and Katri Huitu<sup>3,‡</sup>

<sup>1</sup>*Institute of Physics, Bhubaneswar, Sachivalaya Marg, Sainik School, Bhubaneswar 751005, India*

<sup>2</sup>*Homi Bhabha National Institute, Training School Complex, Anushakti Nagar, Mumbai 400094, India*

<sup>3</sup>*Department of Physics, and Helsinki Institute of Physics, University of Helsinki, Finland 00014*

While the triplet-like Higgses up to a few hundred GeV masses are already excluded for a vast region of the model parameter space from the LHC searches, strikingly, there is a region of this parameter space that is beyond the reach of the existing LHC searches, and doubly/singly-charged and neutral Higgses as light as 200 GeV or even lighter are still allowed by the LHC data. We study several search strategies targeting different parts of this LHC elusive parameter space at two configurations of  $e^-e^+$  colliders—500 GeV and 1 TeV centre of mass energies. We find that a vast region of this parameter space could be probed with  $5\sigma$  discovery with the early  $e^-e^+$  colliders' data.

## I. Introduction

Among several observational and theoretical lacunae of the SM, the discovery of neutrino oscillations—necessitating the neutrinos to be massive—has provided arguably the most irrefutable reason for going beyond the SM. The widely-studied type-II see-saw model [1–6], one of the three UV completions of the so-called Weinberg operator [7] at the tree-level [8], extending the SM with  $SU(2)_L$  triplet scalar field with hypercharge  $Y = 1$  offers a well-founded rationale for the observed neutrino masses and mixings.

Copious production of the triplet-like physical Higgses, *viz.* doubly- and singly-charged Higgses ( $H^{\pm\pm}$  and  $H^\pm$ ) and CP-even and CP-odd neutral Higgses ( $H^0$  and  $A^0$ ), and their eventual decays to the SM fermions and bosons offer interesting ways to probe them directly at colliders. Phenomenology of these states, in particular, the doubly-charged ones, has been studied extensively at the Large Hadron Collider (LHC) [9–41],  $e^-e^+$  colliders [42–46] and  $e^-p$  collider [47, 48]; see Refs. [49, 50] for comprehensive reviews. The observations being consistent with the SM expectations, several LHC searches performed by the CMS and ATLAS collaborations have put stringent limits on them [51–60]. For  $H^{\pm\pm}$  decaying exclusively into same-sign lepton pair, the CMS multilepton search in Ref. [56] has set a limit of 535–820 GeV. The ATLAS multilepton search in Ref. [57] has set a limit of 770–870 GeV and 450 GeV for  $H^{\pm\pm}$  decaying, respectively, 100% and 10% into same-sign light lepton pair. For  $H^{\pm\pm}$  decaying exclusively into same-sign  $W$ -boson pair, the ATLAS search in Ref. [60] has set a limit of 350 GeV and 230 GeV, respectively, for the pair and associated production modes.

Understandably, the LHC searches being designed to probe specific parts of the parameter space defined by the doubly-charged Higgs mass ( $m_{H^{\pm\pm}}$ ), the mass-splitting between the doubly- and singly-charged Higgses ( $\Delta m = m_{H^{\pm\pm}} - m_{H^\pm}$ ) and the triplet vacuum expectation value ( $v_t$ ), the resulted limits are not applicable for the entire parameter space. Ref. [41], incorporating all the relevant productions and decays for the triplet-like Higgses, has derived the most stringent limit at 95% confidence level on  $m_{H^{\pm\pm}}$  for a vast range of  $v_t$ - $\Delta m$  parameter space by recasting several searches by CMS and ATLAS. It has been shown in Ref. [41] that while the triplet-like Higgses up to a few hundred GeV

masses are already excluded for  $\Delta m = 0$  and  $\Delta m < 0$  from the LHC searches, strikingly, there is a region of the parameter space—with large enough positive  $\Delta m$  and moderate  $v_t$ —that is beyond the reach of the existing LHC searches, and Higgses as light as 200 GeV or even lighter are still allowed by the LHC data. The challenges in probing this part of the parameter space at the LHC arise because the charged Higgses decay exclusively to the neutral ones and off-shell  $W$ -bosons resulting in soft hadrons or leptons, which are challenging to reconstruct at the LHC. Thus, charged Higgses' productions only enhance the production of neutral Higgses, which then decay into neutrinos or  $b\bar{b}, t\bar{t}, ZZ, Zh, hh$ , thereby resulting in final states that are challenging to probe at the LHC owing to the towering SM backgrounds. However, future lepton colliders [61–64] are expected to have better prospects for probing this region of parameter space owing to a cleaner environment. This work studies several search strategies targeting different parts of the above-mentioned LHC elusive parameter space at future  $e^-e^+$  colliders. To this end, we consider two configurations of  $e^-e^+$  colliders—500 GeV and 1 TeV centre of mass energies ( $\sqrt{s}$ ).

The rest of this work is structured as follows. In Section II, we briefly discuss the type-II see-saw model and the productions and decays of the triplet-like Higgses. We perform a comprehensive collider analysis for them in several final states at the 500 GeV and 1 TeV  $e^-e^+$  colliders in Section III. Finally, we summarise in Section IV.

## II. The Higgs triplet

In addition to the SM field content, the type-II see-saw model employs a  $SU(2)_L$  triplet scalar field with  $Y = 1$ :

$$\Delta = \begin{pmatrix} \Delta^+/\sqrt{2} & \Delta^{++} \\ \Delta^0 & -\Delta^+/\sqrt{2} \end{pmatrix}.$$

The scalar potential involving  $\Delta$  and the SM Higgs doublet  $\Phi = (\Phi^+ \ \Phi^0)^T$  is given by [65]

$$\begin{aligned} V(\Phi, \Delta) = & -m_\Phi^2 \Phi^\dagger \Phi + \frac{\lambda}{4} (\Phi^\dagger \Phi)^2 + m_\Delta^2 \text{Tr}(\Delta^\dagger \Delta) \\ & + [\mu (\Phi^T i\sigma^2 \Delta^\dagger \Phi) + \text{h.c.}] + \lambda_1 (\Phi^\dagger \Phi) \text{Tr}(\Delta^\dagger \Delta) \\ & + \lambda_2 [\text{Tr}(\Delta^\dagger \Delta)]^2 + \lambda_3 \text{Tr}[(\Delta^\dagger \Delta)^2] + \lambda_4 \Phi^\dagger \Delta \Delta^\dagger \Phi, \end{aligned}$$

where  $m_\Phi^2, m_\Delta^2$  and  $\mu$  are the mass parameters,  $\lambda$  and  $\lambda_i$  ( $i = 1, \dots, 4$ ) are the dimensionless quartic couplings. The neutral components of  $\Phi$  and  $\Delta$  can be parametrised as  $\Phi^0 = (v_d + h + iZ_1)/\sqrt{2}$  and  $\Delta^0 = (v_t + \xi + iZ_2)/\sqrt{2}$ , where

\* [saiyad.a@iopb.res.in](mailto:saiyad.a@iopb.res.in)

† [kirti.gh@gmail.com](mailto:kirti.gh@gmail.com)

‡ [katri.huitu@helsinki.fi](mailto:katri.huitu@helsinki.fi)

$v_d$  and  $v_t$  are their respective vacuum expectation values (VEVs) with  $\sqrt{v_d^2 + 2v_t^2} = 246$  GeV. After the electroweak symmetry is broken, the degrees of freedom carrying identical electric charges mix, thereby resulting in several physical Higgs states:

- (i) the neutral states  $\Phi^0$  and  $\Delta^0$  mix into two CP-even states ( $h$  and  $H^0$ ) and two CP-odd states ( $G^0$  and  $A^0$ ),
- (ii) the singly-charged states  $\Phi^\pm$  and  $\Delta^\pm$  mix into two mass states  $G^\pm$  and  $A^\pm$ ,
- (iii) the doubly-charged gauge state  $\Delta^{\pm\pm}$  is aligned with its mass state  $H^{\pm\pm}$ .

The mass states  $G^0$  and  $G^\pm$  are the so-called *would-be* Nambu-Goldstone bosons eaten by the longitudinal modes of  $Z$  and  $W^\pm$ , and the rest of them are massive with  $h$  being identified as the 125-GeV resonance observed at the LHC.

The Yukawa interaction  $Y_{ij}^\nu L_i^T C i \sigma^2 \Delta L_j$  of the triplet Higgs with the SM lepton doublet leads to the non-zero masses for the neutrinos after the electroweak symmetry breaking ( $Y^\nu$  is a  $3 \times 3$  symmetric complex matrix,  $i$  and  $j$  are the generation indices, and  $C$  is the charge-conjugation matrix):

$$m_\nu = \sqrt{2} Y^\nu v_t.$$

Consequently,  $Y^\nu$  is determined by the neutrino oscillation parameters up to the triplet VEV. In this work, we take the best fit values for the neutrino oscillation parameters from Ref. [66] except for the Dirac and Majorana phases which we set to zero for simplicity.

In this model, there are only three phenomenologically relevant parameters, namely the doubly-charged Higgs mass ( $m_{H^{\pm\pm}}$ ), the mass-splitting between the doubly- and singly-charged Higgses ( $\Delta m = m_{H^{\pm\pm}} - m_{H^\pm}$ ) and  $v_t$ . The triplet-like singly-charged and neutral Higgs masses are given by

$$m_{H^\pm} = m_{H^{\pm\pm}} - \Delta m \text{ and } m_{H^0/A^0} \approx \sqrt{m_{H^{\pm\pm}}(m_{H^{\pm\pm}} - 4\Delta m)}.$$

For the sake of completeness, we briefly mention the relevant constraints on them.

- (i) The value of the  $\rho$  parameter from the electroweak precision data (EWPD) [67] leads to an upper bound of  $\mathcal{O}(1)$  GeV on  $v_t$ .
- (ii) The EWPD observables, *viz.*  $S, T$  and  $U$  parameters robustly constrain the mass-splittings requiring  $|\Delta m| \lesssim 40$  GeV [38, 68–70].
- (iii) The upper limits on the lepton flavour violating decays  $\mu^- \rightarrow e^- \gamma$  [71] and  $\mu^- \rightarrow e^+ e^- e^-$  [72] tightly constrain the  $v_t$ - $m_{H^{\pm\pm}}$  parameter space [73–75]:

$$v_t \gtrsim \mathcal{O}(10^{-9}) \text{ GeV} \times \frac{1 \text{ TeV}}{m_{H^{\pm\pm}}}.$$

- (iv) For  $\Delta m = 0$  and large (small)  $v_t$ , doubly charged scalars with masses below 420(955) GeV are excluded from the LHC searches [41]. For large enough negative  $\Delta m$  and moderate  $v_t$ , the exclusion limit extends up to 1115 GeV. However, for large enough positive  $\Delta m$  and moderate  $v_t$ , triplet-like Higgses as light as 200 GeV or even lighter are still allowed by the LHC data.

The triplet Higgses can be pair produced aplenty at  $e^- e^+$

colliders through  $s$ -channel  $\gamma/Z$  exchanges [45]:<sup>1</sup>

$$e^- e^+ \rightarrow H^{++} H^{--}, H^+ H^-, H^0 A^0.$$

We evaluate the leading order production cross-sections using the SARAH [76, 77] generated UFO [78] modules in MadGraph [79, 80]. Fig. 1 shows the total production cross-sections for the triplet-like Higgses as a function of  $m_{H^{\pm\pm}}$  for  $\Delta m = 30$  GeV at both the 500 GeV and 1 TeV  $e^- e^+$  colliders.

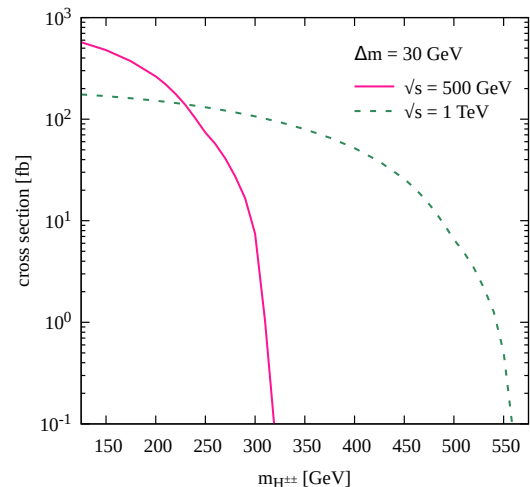


FIG. 1. Total production cross-sections for the triplet-like Higgses at the 500 GeV and 1 TeV  $e^- e^+$  colliders.

After being produced, the triplet-like Higgses decay either to a lighter triplet-like Higgs and an off-shell  $W$ -boson or a pair of SM particles. For the model parameter space of our interest—with large enough positive  $\Delta m$  and moderate  $v_t$ ,  $H^{\pm\pm}$  and  $H^\pm$  undergo the former decay, thereby enhancing the productions of  $H^0$  and  $A^0$  effectively. Finally,  $H^0$  and  $A^0$  decay into a pair of neutrinos or/and  $b\bar{b}, t\bar{t}, ZZ, Zh, hh$ . In Fig. 2, we present their branching fractions as a function of  $v_t$  for different values of  $m_{H^{\pm\pm}}$ —200, 250, 350 and 450 GeV with  $\Delta m = 30$  GeV. As these plots suggest, the dominance of a decay mode over the others depends, naturally, on their mass and  $v_t$ . For instance, for  $v_t > \mathcal{O}(10^{-4})$  GeV, while a light  $H^0/A^0$  decay dominantly into  $b\bar{b}$ , the heavier  $A^0(H^0)$  decay into  $Zh$  ( $WW$  and  $hh$ ). For  $v_t < \mathcal{O}(10^{-4})$  GeV, they decay exclusively into a pair of neutrinos irrespective of their mass.

### III. Collider phenomenology

Abundant production of the triplet-like Higgses followed by their eventual decays to the SM particles will lead to various final state signatures at  $e^- e^+$  colliders. Led the way by the decay patterns of  $H^0$  and  $A^0$ , we define several signal regions (SRs) targeting different parts of the above-mentioned parameter space, see Table I (and the corresponding benchmark points are summarised in Table II). Before going into the SR-specific selection, we briefly describe the reconstruction and selection of various physics objects.

<sup>1</sup> They can also be single or pair produced via vector boson-fusion processes with two associated forward leptons at  $e^- e^+$  colliders. However, we do not consider these due to their small contribution.

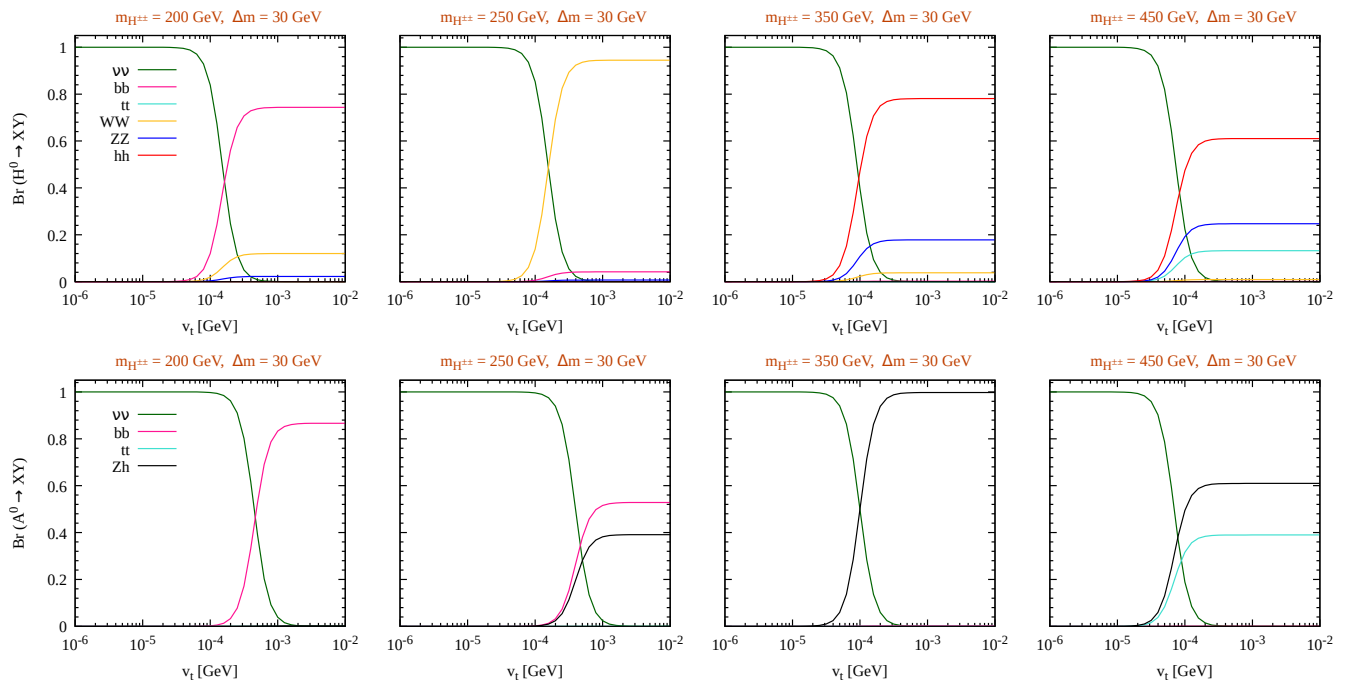


FIG. 2. Branching fractions for the triplet-like CP-even (top panel) and CP-odd (bottom panel) neutral Higgses.

SR	parameter space of interest			Final state of interest	$\sqrt{s}$ (GeV)
	$v_t$ (GeV)	$\Delta m$ (GeV)	$m_{H^{\pm\pm}}$ (GeV)		
SR1	$\gtrsim \mathcal{O}(10^{-4})$	30	$\lesssim 250$	$\geq 2b$ -jets + anything	500
SR2	$\mathcal{O}(10^{-4}) - \mathcal{O}(10^{-3})$	30	$\lesssim 290$	$\geq 3$ jets + $p_T^{\text{miss}}$	500
SR3	$\gtrsim \mathcal{O}(10^{-4})$	30	$\gtrsim 250(500)$	soft leptons/jets	500(1000)
SR4	$\gtrsim \mathcal{O}(10^{-4})$	30	250–550	$\geq 7$ jets	1000

TABLE I. SRs targeting different parts of the parameter space.

SR	Benchmark points			
	name	$m_{H^{\pm\pm}}$ (GeV)	$\Delta m$ (GeV)	$v_t$ (GeV)
SR1	<i>BP1</i>	230	30	$3 \times 10^{-4}$
SR2	<i>BP2</i>	260	30	$3 \times 10^{-4}$
SR3	<i>BP3 (BP4)</i>	240 (425)	30	$10^{-5}$
SR4	<i>BP5</i>	375	30	$3 \times 10^{-4}$

TABLE II. Benchmark points used for different SRs.

## A. Object reconstruction and selection

We use `MadGraph` [79, 80] to simulate parton-level events for both signals and backgrounds. We pass those events into `PYTHIA` [81] to simulate subsequent decays for the unstable particles, initial and final state radiations, showering, fragmentation and hadronisation. Finally, we pass them into `Delphes` [82] for simulating detector effects as well as reconstructing various physics objects, *viz.* photons, electrons, muons and jets. Jets are reconstructed using the *anti- $k_T$*  algorithm [83] with a characteristic radius 0.4 in `FastJet` [84]. Jets (leptons, *i.e.* electrons and muons, and photons) are required to be within the pseudorapidity range  $|\eta| < 2.4(2.5)$  and have a transverse momentum  $p_T > 10(5)$  GeV. Further,

muons (photons and electrons) are required to be isolated, and this is ensured by demanding the scalar sum of the  $p_T$ s of all other objects lying within a cone of radius 0.5 around it to be smaller than 15%(12%) of its  $p_T$ . Such stringent isolation requirements significantly suppress the reducible backgrounds. Finally, the missing transverse momentum vector  $\vec{p}_T^{\text{miss}}$  (with magnitude  $p_T^{\text{miss}}$ ) is estimated from the momentum imbalance in the transverse direction associated to all reconstructed objects in an event.

## B. SM Backgrounds

While different SM processes serve as the main background for different SRs, for the sake of completeness, we consider all the relevant backgrounds across the SRs. These include diboson ( $VV$  with  $V$  denoting the gauge bosons), triboson ( $VVV$ ) and tetraboson ( $VVVV$ ) productions, Higgsstrahlung processes ( $Vh$ ,  $VVh$ ,  $Vhh$ ,  $tth$ ), multi-top production ( $t\bar{t}$ ,  $t\bar{t}t$ ), top-pair production in association with gauge bosons ( $t\bar{t}V$ ,  $t\bar{t}VV$ ), dilepton production and multi-jet production.

## C. SR-specific event selection

We now briefly discuss the SR-specific selection criteria that would significantly suppress the background without impinging much on the signal. To achieve this, we use various kinematic distributions as a guiding premise.

### 1. SR1: $v_t \gtrsim \mathcal{O}(10^{-4})$ , $\Delta m \sim 30$ , $m_{H^{\pm\pm}} \lesssim 250$ GeV

In this SR,  $A^0$  dominantly decays into  $b\bar{b}$ , and  $H^0$  decays to  $\nu\nu$ ,  $b\bar{b}$  or  $WW$  so that the final state includes at least two  $b$ -jets in addition to other jets or leptons if any. We require at least two of the jets to be  $b$ -tagged. The invariant mass distribution of these two  $b$ -tagged jets are expected to peak at  $m_{H^0/A^0}$ . The SM processes  $t\bar{t}$  and  $b\bar{b}$  serve as the main

irreducible backgrounds for this final state. In Fig. 3, we display two normalised kinematic distributions for the signal and background events at the 500 GeV  $e^-e^+$  collider. The signal events are shown for a benchmark point *BP1*:  $m_{H^{\pm\pm}} = 230$  GeV,  $\Delta m = 30$  GeV and  $v_t \sim 3 \times 10^{-4}$  GeV. The left plot shows the distribution for the angle between the two  $b$ -tagged jets ( $\cos\theta_{bb}$ ). In case of more than two  $b$ -tagged jets, the pair with maximum separation in the azimuth plane is considered. The background boasts a peak around  $\cos\theta_{bb} = -1$  with the most dominant contribution coming from  $b\bar{b}$  events with the pair of  $b$ -jets emanating back-to-back. Displayed in the right plot is the distribution of the sum of all non  $b$ -tagged jet energies ( $E_{\text{light jets}}$ ). To improve the signal-to-background ratio, we impose the following selection cuts:

$$\cos\theta_{bb} \in [-0.96, 0.4] \text{ and } E_{\text{light jets}} < 250 \text{ GeV.}$$

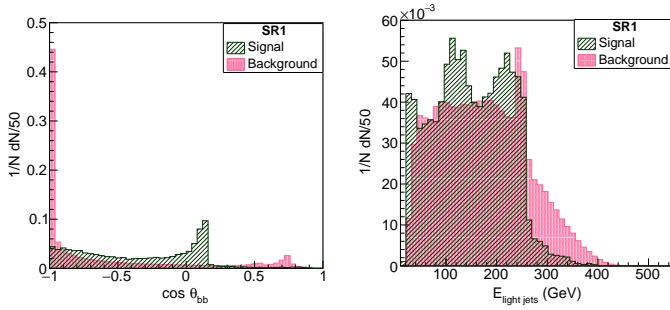


FIG. 3. Normalised kinematic distributions for the signal (*BP1*) and background at the 500 GeV  $e^-e^+$  collider. Left:  $\cos\theta_{bb}$  and right:  $E_{\text{light jets}}$ .

The sensitivity of this search is increased by dividing the selected events into 8 bins in the range [100,300] GeV using the invariant mass of the two  $b$ -tagged jets ( $m_{bb}$ ) as the final discriminating variable between the signal and background (see Fig. 4). As we expected, the  $m_{bb}$  distribution peaks in the 150–175 GeV bin, thereby reconstructing the triplet-like neutral Higgses.

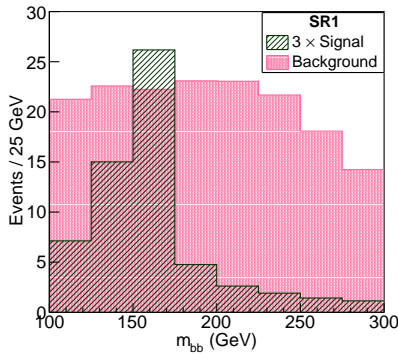


FIG. 4.  $m_{bb}$  distribution for the signal (*BP1*) and background. The events are weighted for  $1 \text{ fb}^{-1}$  luminosity at the 500 GeV  $e^-e^+$  collider.

## 2. SR2: $v_t \sim \mathcal{O}(10^{-4})\text{--}\mathcal{O}(10^{-3})$ , $\Delta m \sim 30$ , $m_{H^{\pm\pm}} \lesssim 290$ GeV

In this SR, one of  $A^0$  and  $H^0$  decays into  $\nu\nu$ , and the other decays to  $WW$  or  $Zh$ . We require at least three jets

in the final state. To suppress the background contributions from  $t\bar{t}$  and  $b\bar{b}$  processes, we apply a  $b$ -jet veto. We display some normalised kinematic distributions for the signal and background events at the 500 GeV  $e^-e^+$  collider in Fig. 5. The signal events are shown for a benchmark point *BP2*:  $m_{H^{\pm\pm}} = 260$  GeV,  $\Delta m = 30$  GeV and  $v_t \sim 3 \times 10^{-4}$  GeV. The left (middle) plot shows the distribution for the sum of all jet (lepton) energies,  $E_{\text{jets}}$  ( $E_{\text{leptons}}$ ). As for the  $E_{\text{jets}}$  distribution for the background events, it is almost a monotonically rising one, peaking at  $\sqrt{s}$ , with most of the contributions coming from  $WW$  and  $t\bar{t}$  productions. Whereas for the signal events, it is a wide one, extending up to  $\sqrt{s}$  with a peak at  $\sqrt{s}/2$ . Also displayed, in the right plot, is the  $p_T^{\text{miss}}$  distribution. For the signal, this distribution is almost flat, extending beyond 150 GeV. This is effectuated by one of the two triplet-like scalars' decay into hadronic final state, with the other decaying invisibly. On the contrary, for the background events, it is almost a monotonically falling one, falling sharply at very low  $p_T^{\text{miss}}$ . Guided by these kinematic distributions, we impose the following selection cuts to improve the signal-to-background ratio:

$$E_{\text{jets}} < 260 \text{ GeV, } E_{\text{leptons}} < 120 \text{ GeV and } p_T^{\text{miss}} > 40 \text{ GeV.}$$

Though the adoption of the cut on  $E_{\text{jets}}$  impinges on the signal strength, this significantly increases the signal-to-background ratio, owing to a much diminished background.

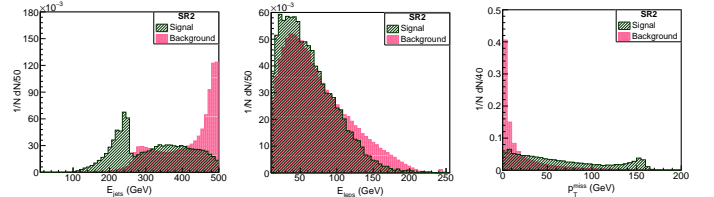


FIG. 5. Normalised kinematic distributions for the signal (*BP2*) and background at the 500 GeV  $e^-e^+$  collider. Left:  $E_{\text{jets}}$ , middle:  $E_{\text{leptons}}$  and right:  $p_T^{\text{miss}}$ .

To enhance the sensitivity of this search further, the selected events are distributed over 8 bins in the range [50,250] GeV using the invariant mass of all jets,  $m_{\text{jets}}$  (see Fig. 6).

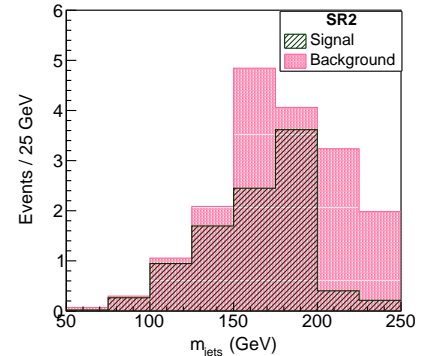


FIG. 6.  $m_{\text{jets}}$  distribution for the signal (*BP2*) and background. The events are weighted for  $1 \text{ fb}^{-1}$  luminosity at the 500 GeV  $e^-e^+$  collider.



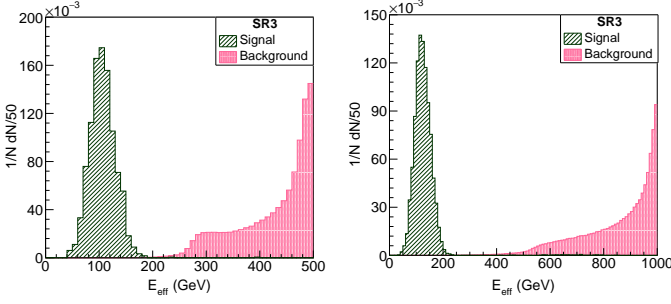


FIG. 7. Normalised  $E_{\text{eff}}$  distribution for the signal (left:  $BP_3$ , right:  $BP_4$ ) and background at the 500 GeV (left) and 1 TeV (right)  $e^-e^+$  colliders.

### 3. SR3: $v_t \lesssim \mathcal{O}(10^{-4})$ , $\Delta m \sim 30$ and $m_{H^{\pm\pm}} \lesssim 500$ GeV

In this SR,  $H^{\pm\pm}$  and  $H^\pm$  decay to  $H^0/A^0$  and off-shell  $W$ -bosons. While  $H^0$  and  $A^0$  decay into neutrinos, the off-shell  $W$ -bosons decay into soft leptons/jets, thereby resulting into soft leptons/jets plus  $p_T^{\text{miss}}$  in the final state. We require at least three soft leptons and/or jets in the final state. In Fig. 7, we display the normalised kinematic distributions for  $E_{\text{eff}} = E_{\text{jets}} + E_{\text{leptons}} + p_T^{\text{miss}}$  for the signal and background events at the 500 GeV and 1 TeV  $e^-e^+$  colliders. The signal events are shown for a benchmark point  $BP_3$  ( $BP_4$ ):  $m_{H^{\pm\pm}} = 240(425)$  GeV,  $\Delta m = 30$  GeV and  $v_t \sim 10^{-5}$  GeV at the 500 GeV (1 TeV) collider. For the signal, this distribution boasts a peak around 100 GeV, thereafter falling sharply. This is occasioned by the softness of the leptons/jets stemming from the off-shell  $W$ -bosons. On the other hand, for the background events, it is almost a monotonically rising one, peaking at  $\sqrt{s}$ , with bulk of the contributions coming from  $WW$ ,  $ZZ$  and  $t\bar{t}$  productions. Guided by these distributions, we apply the following selection cut to ameliorate the signal-to-background ratio:

$$E_{\text{eff}} < 200(250) \text{ GeV for the 500 GeV (1 TeV) collider.}$$

Finally, the selected events are distributed over 7 bins in the range  $[0,175]$  GeV using the transverse mass  $m_T$  (see Fig. 8), where  $m_T$  is defined as

$$m_T^2 = 2p_T^{\text{miss}} p_T^{\text{vis}} \left( 1 - \cos \Delta\phi_{\vec{p}_T^{\text{miss}}, \vec{p}_T^{\text{vis}}} \right),$$

where  $\vec{p}_T^{\text{vis}}$  (with magnitude  $p_T^{\text{vis}}$ ) is the vector sum of the transverse momenta of all leptons and jets, and  $\Delta\phi_{\vec{p}_T^{\text{miss}}, \vec{p}_T^{\text{vis}}}$  is the azimuthal separation between  $\vec{p}_T^{\text{miss}}$  and  $\vec{p}_T^{\text{vis}}$ .

### 4. SR4: $v_t \gtrsim \mathcal{O}(10^{-4})$ , $\Delta m \sim 30$ , $m_{H^{\pm\pm}} \sim 250\text{--}550$ GeV

In this SR,  $H^0$  and  $A^0$  decay dominantly into  $hh/ZZ$  and  $Zh$ , respectively. Thus, we have  $hhhZ$  or  $ZZZh$  in the final state, in addition to the off-shell  $W$ -bosons coming from the cascade decays of  $H^{\pm\pm}$  and  $H^\pm$ . The hadronic decays of the  $Z/h$ -bosons results in up to eight jets in addition to the soft leptons/jets coming from the off-shell  $W$ -bosons. We require at least seven jets in the final state, with at least two of them to be  $b$ -tagged. This requirement reduces the background contributions from the diboson and QCD jets (in particular,  $b\bar{b}$ +jets) production processes to a negligible level, while keeping only a small fraction of contributions from the triboson and multi-top production processes. Brushing aside the

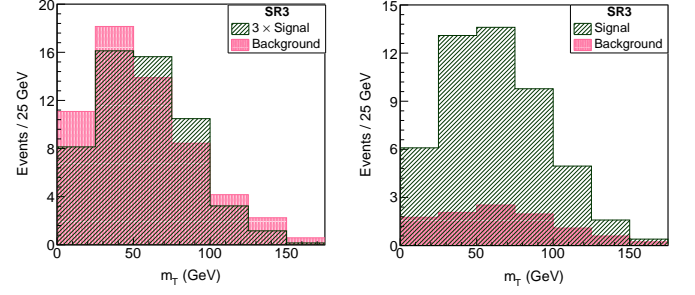


FIG. 8.  $m_T$  distribution for the signal (left:  $BP_3$ , right:  $BP_4$ ) and background. The events are weighted for  $10 \text{ fb}^{-1}$  luminosity at the 500 GeV (left) and 1 TeV (right)  $e^-e^+$  colliders.

soft jets/leptons from the off-shell  $W$ -bosons, there are as many as eight hard jets in the final state, in addition to the others coming from radiations and pileup interactions. On account of the high-multiplicity signature in the final state, it is particularly burdensome to correctly associate the reconstructed jets in an event with the elementary quarks of that event topology. This makes the kinematic reconstruction of  $H^0/A^0$  very challenging. To resolve this *combinatorial problem*, we use the so-called  $\chi^2$ -minimisation method, *i.e.* by enumerating and evaluating all possible permutations in an event, we identify the *best* assignment through minimising the objective function

$$\chi^2 = \frac{(m_{j_1 j_2} - m_{h/Z})^2}{m_{h/Z}^2} + \frac{(m_{j_3 j_4} - m_{h/Z})^2}{m_{h/Z}^2} + \frac{(m_{j_5 j_6} - m_{h/Z})^2}{m_{h/Z}^2} + \frac{(m_{j_7 j_8} - m_{h/Z})^2}{m_{h/Z}^2} + \frac{(m_{j_1 j_2 j_3 j_4} - m_{j_5 j_6 j_7 j_8})^2}{\sigma_{H/A}^2},$$

and

$$\chi^2 = \frac{(m_{j_1 j_2} - m_{h/Z})^2}{m_{h/Z}^2} + \frac{(m_{j_3 j_4} - m_{h/Z})^2}{m_{h/Z}^2} + \frac{(m_{j_5 j_6} - m_{h/Z})^2}{m_{h/Z}^2} + \frac{(m_{j_1 j_2 j_3 j_4} - m_{j_5 j_6 j_7 j_8})^2}{\sigma_{H/A}^2},$$

respectively, for eight and seven jet events with the jets being denoted as  $j_1, j_2, \dots, j_8$ ,  $\sigma_{H/A} = (m_{j_1 j_2 j_3 j_4} + m_{j_5 j_6 j_7 j_8})/2$  and  $\sigma'_{H/A} = (m_{j_1 j_2 j_3 j_4} + m_{j_5 j_6 j_7})/2$ . This method requires enumeration and evaluation of 315 (360) distinct permutations for eight (seven) jet events. In Fig. 9, we display the normalised invariant mass distributions for the *best-assigned*<sup>2</sup> jet pairs for the signal and background events at the 1 TeV  $e^-e^+$  collider. The signal events are shown for a benchmark point  $BP_5$ :  $m_{H^{\pm\pm}} = 375$  GeV,  $\Delta m = 30$  GeV and  $v_t \sim 3 \times 10^{-4}$  GeV. The effectiveness of the  $\chi^2$ -minimisation method has been exemplified by these distributions, each boasting two peaks—one at  $m_Z$  and the other at  $m_h$ , thereby reasonably reconstructing the  $h$ - and  $Z$ -bosons in the signal final state. However, note that not only does this method cost a considerable time, but also it obscures the kinematic reconstruction owing to the incorrect assignments of the reconstructed jets to the particles in the event topology.

<sup>2</sup> The jet pairs' assignment corresponding to the minimum objective function is referred to as the *best* assignment.

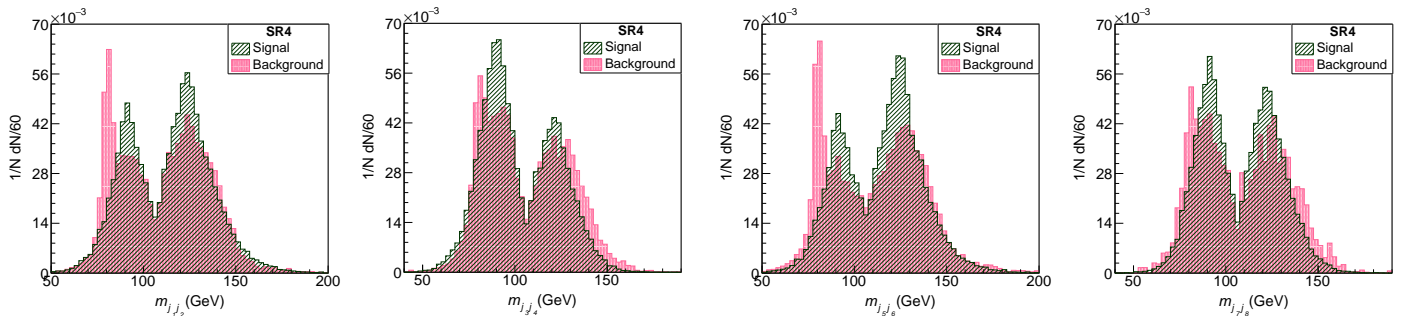


FIG. 9. Normalised invariant mass distributions for the *best-assigned* jet pairs for the signal (*BP5*) and background at the 1 TeV  $e^-e^+$  collider.

Finally,  $H^0/A^0$  can be kinematically reconstructed from two pairs of jets in an event:

$$M_{\text{inv}} = (m_{j_1 j_2 j_3 j_4} + m_{j_5 j_6 j_7 j_8})/2,$$

and

$$M_{\text{inv}} = m_{j_1 j_2 j_3 j_4},$$

respectively, for 8 and 7 jet events. The sensitivity of this search is increased further by distributing the selected events into 9 bins in the range [160,520] GeV using the invariant mass  $M_{\text{inv}}$  (see Fig. 10). As we expected, the  $M_{\text{inv}}$  distribution peaks in the 280–320 GeV bin, thereby reconstructing the  $H^0/A^0$ .

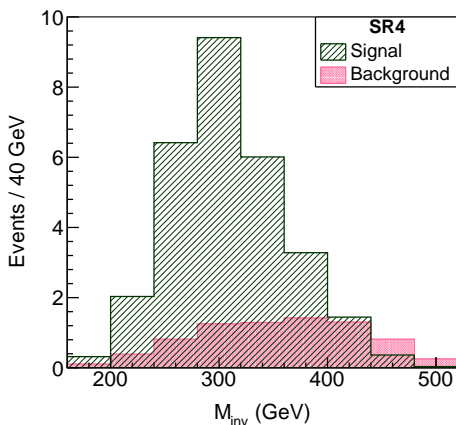


FIG. 10.  $M_{\text{inv}}$  distribution for the signal (*BP5*) and background. The events are weighted for 1  $\text{fb}^{-1}$  luminosity at the 1 TeV  $e^-e^+$  collider.

#### D. Discovery reach

Next, we estimate the discovery reaches of the above searches by using a hypothesis tester named **Profile Likelihood Number Counting Combination**, which uses a library of C++ classes **RooFit** [85] in the **ROOT** [86] environment. Without going into the intricacy of estimating the background uncertainties, we assume an overall 5% total uncertainty on the estimated background. In Fig. 11, we project the required luminosities for 5 $\sigma$  discovery of the triplet-like Higgses as a function of their mass in different SRs at the 500 GeV and 1 TeV  $e^-e^+$  colliders. Also shown, in

Fig. 12, are the discovery reaches for the triplet-like Higgses in the  $v_t$ - $m_{H^{\pm\pm}}$  plane in different SRs at two configurations of  $e^-e^+$  colliders—500 GeV and 1 TeV  $e^-e^+$  colliders, respectively, with 500 and 1000  $\text{fb}^{-1}$  luminosity data. For the sake of completeness, we also show the regions that are excluded from the LHC run 2 searches at 95% confidence level (shaded in dark gray) or expected to be probed at the HL-LHC (shaded in peach) [41]. For the 500 GeV  $e^-e^+$  configuration with 500  $\text{fb}^{-1}$  data, *SR2* has the maximum discovery reach of  $m_{H^{\pm\pm}} \sim 285$  GeV because of its small background, whereas a considerably large background for both *SR1* and *SR3* limits its discovery reach to  $m_{H^{\pm\pm}} \sim 245$  GeV. Likewise, for the 1 TeV  $e^-e^+$  configuration with 1000  $\text{fb}^{-1}$  data, *SR4* is the most promising signal region with the discovery reach of  $m_{H^{\pm\pm}} \sim 535$  GeV because of its small background and ability to kinematically reconstruct the neutral Higgses  $H^0/A^0$ , and *SR3* has a discovery reach of  $m_{H^{\pm\pm}} \sim 485$  GeV.

#### IV. Summary and outlook

While the triplet-like Higgses up to a few hundred GeV masses are already excluded for a vast region of the model parameter space from the LHC searches, strikingly, there is a region of this parameter space—with large enough positive mass-splitting between the doubly- and singly-charged Higgses and moderate triplet Higgs scalar vacuum expectation value—that is beyond the reach of the existing LHC searches, and such Higgses as light as 200 GeV or even lighter are still allowed by the LHC data [41]. In this region of the parameter space, the charged Higgses decay exclusively to the neutral ones and off-shell  $W$ -bosons. The latter results in soft leptons/jets that are challenging to reconstruct at the LHC. Furthermore, the neutral Higgses decay into neutrinos or  $b\bar{b}$ ,  $t\bar{t}$ ,  $ZZ$ ,  $Zh$ ,  $hh$ , thereby resulting in final states that are challenging to probe at the LHC owing to the towering SM backgrounds. However, owing to a cleaner environment, future lepton colliders are expected to have better prospects for probing this LHC elusive parameter space. In this work, we study several search strategies targeting different parts of this parameter space at future  $e^-e^+$  colliders with 500 GeV and 1 TeV centre of mass energies. We find that a vast region of this parameter space, with some parts of this—parametrised by *SR1* and *SR4* signal regions—allowing for kinematic reconstructions of the triplet-like neutral Higgses, could be probed with 5 $\sigma$  discovery with the early  $e^-e^+$  colliders' data. In closing this section, here are a few comments in order. (i) For the sake of definiteness, we have shown

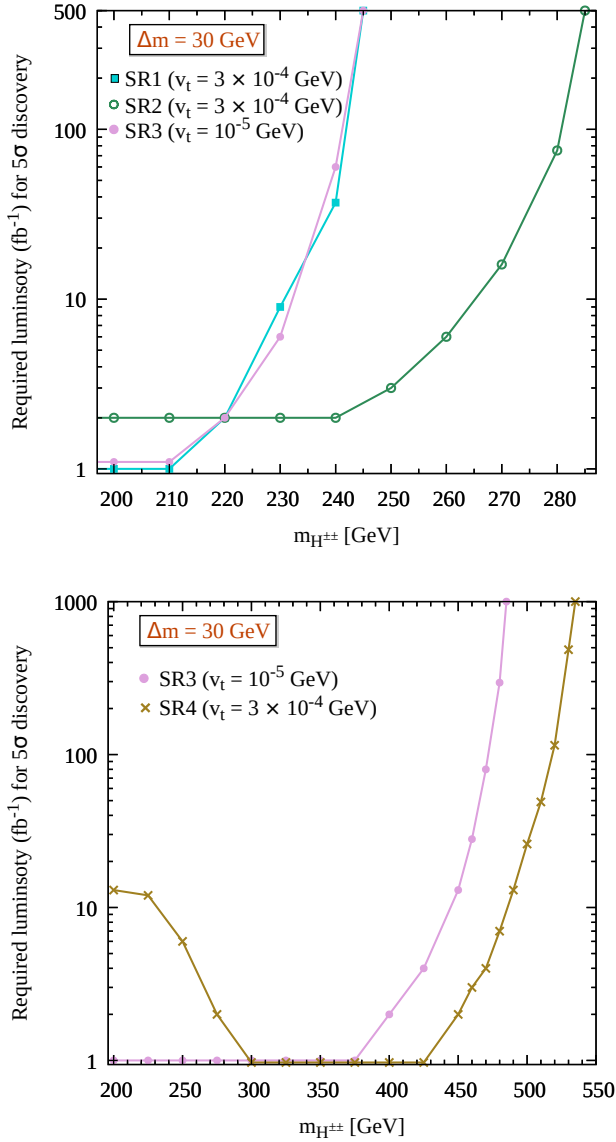


FIG. 11. Required luminosity for  $5\sigma$  discovery of the triplet-like Higgses in different SRs at the 500 GeV (top) and 1 TeV (bottom)  $e^-e^+$  colliders.

our findings for a mass-splitting of 30 GeV. However, the searches presented above would also be sensitive for smaller mass-splittings. Brushing aside a little quantitative difference in production cross-sections for the triplet-like Higgses, the only major difference between a smaller mass-splitting (say, 10 GeV) and a larger one (say, 30 GeV) is that the leptons/jets stemming from the off-shell  $W$ -bosons would be softer. Note that only the search in SR3 targets soft leptons/jets in the final state. Therefore, for a smaller mass-splitting, the  $E_{\text{eff}}$  distribution in Fig. 7 would shift towards lower values, thus, allowing one to impose a stronger cut on it. While this would impinge only a little on the signal strength, the same would significantly enhance the signal-to-background ratio, primarily on account of a much reduced background. On the other hand, the searches in SR1, SR2 and SR4 targets hard jets/leptons stemming from the triplet-like Higgses' decays, thus these are almost independent of the mass-splitting. (ii) The SR3 region of parameter space could

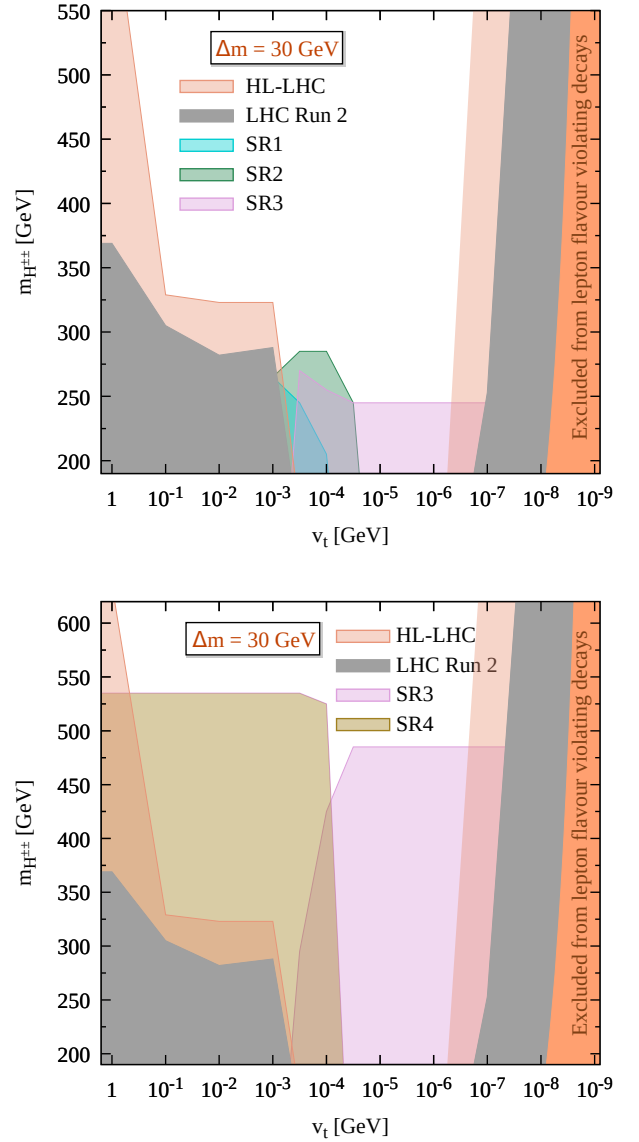


FIG. 12. Summary of the discovery reaches for the triplet-like Higgses in different SRs at the 500 GeV (top) and 1 TeV (bottom)  $e^-e^+$  colliders with 500 and 1000  $\text{fb}^{-1}$  luminosity data, respectively. The dark gray and peach shaded regions are taken from Ref. [41]. See text for details.

also be probed by using a search with a photon and missing transverse momentum in the final state. Such a final states suffer from a large irreducible background contributions from the  $t$ -channel  $W$ -exchange process  $\nu\bar{\nu}\gamma$ . Though this background could be reduced by a factor of few by using polarised beams (positive for  $e^-$  and negative for  $e^+$ ), on account of the small signal strength occasioned by the requirement of an energetic photon, the discovery reach of such a search would be very limited.

### Acknowledgments

KG acknowledges support from the DST INSPIRE Research Grant [DST/INSPIRE/04/2014/002158] and SERB Core Research Grant [CRG/2019/006831].

## References

- [1] W. Konetschny and W. Kummer, “Nonconservation of Total Lepton Number with Scalar Bosons,” *Phys. Lett. B* **70**, 433–435 (1977).
- [2] T. P. Cheng and L.-F. Li, “Neutrino Masses, Mixings and Oscillations in  $SU(2) \times U(1)$  Models of Electroweak Interactions,” *Phys. Rev. D* **22**, 2860 (1980).
- [3] G. Lazarides, Q. Shafi, and C. Wetterich, “Proton Lifetime and Fermion Masses in an  $SO(10)$  Model,” *Nucl. Phys. B* **181**, 287–300 (1981).
- [4] J. Schechter and J. W. F. Valle, “Neutrino Masses in  $SU(2) \times U(1)$  Theories,” *Phys. Rev. D* **22**, 2227 (1980).
- [5] R. N. Mohapatra and G. Senjanovic, “Neutrino Masses and Mixings in Gauge Models with Spontaneous Parity Violation,” *Phys. Rev. D* **23**, 165 (1981).
- [6] M. Magg and C. Wetterich, “Neutrino Mass Problem and Gauge Hierarchy,” *Phys. Lett. B* **94**, 61–64 (1980).
- [7] S. Weinberg, “Baryon and Lepton Nonconserving Processes,” *Phys. Rev. Lett.* **43**, 1566–1570 (1979).
- [8] E. Ma, “Pathways to naturally small neutrino masses,” *Phys. Rev. Lett.* **81**, 1171–1174 (1998), [arXiv:hep-ph/9805219](#).
- [9] K. Huitu, J. Maalampi, A. Pietila, and M. Raidal, “Doubly charged Higgs at LHC,” *Nucl. Phys. B* **487**, 27–42 (1997), [arXiv:hep-ph/9606311](#).
- [10] J. F. Gunion, C. Loomis, and K. T. Pitts, “Searching for doubly charged Higgs bosons at future colliders,” eConf **C960625**, LTH096 (1996), [arXiv:hep-ph/9610237](#).
- [11] S. Chakrabarti, D. Choudhury, R. M. Godbole, and B. Mukhopadhyaya, “Observing doubly charged Higgs bosons in photon-photon collisions,” *Phys. Lett. B* **434**, 347–353 (1998), [arXiv:hep-ph/9804297](#).
- [12] M. Muhlleitner and M. Spira, “A Note on doubly charged Higgs pair production at hadron colliders,” *Phys. Rev. D* **68**, 117701 (2003), [arXiv:hep-ph/0305288](#).
- [13] A. G. Akeroyd and M. Aoki, “Single and pair production of doubly charged Higgs bosons at hadron colliders,” *Phys. Rev. D* **72**, 035011 (2005), [arXiv:hep-ph/0506176](#).
- [14] T. Han, B. Mukhopadhyaya, Z. Si, and K. Wang, “Pair production of doubly-charged scalars: Neutrino mass constraints and signals at the LHC,” *Phys. Rev. D* **76**, 075013 (2007), [arXiv:0706.0441 \[hep-ph\]](#).
- [15] F. del Aguila and J. A. Aguilar-Saavedra, “Distinguishing seesaw models at LHC with multi-lepton signals,” *Nucl. Phys. B* **813**, 22–90 (2009), [arXiv:0808.2468 \[hep-ph\]](#).
- [16] P. Fileviez Perez, T. Han, G.-y. Huang, T. Li, and K. Wang, “Neutrino Masses and the CERN LHC: Testing Type II Seesaw,” *Phys. Rev. D* **78**, 015018 (2008), [arXiv:0805.3536 \[hep-ph\]](#).
- [17] A. G. Akeroyd and C.-W. Chiang, “Doubly charged Higgs bosons and three-lepton signatures in the Higgs Triplet Model,” *Phys. Rev. D* **80**, 113010 (2009), [arXiv:0909.4419 \[hep-ph\]](#).
- [18] A. G. Akeroyd, C.-W. Chiang, and N. Gaur, “Leptonic signatures of doubly charged Higgs boson production at the LHC,” *JHEP* **11**, 005 (2010), [arXiv:1009.2780 \[hep-ph\]](#).
- [19] A. Melfo, M. Nemevsek, F. Nesti, G. Senjanovic, and Y. Zhang, “Type II Seesaw at LHC: The Roadmap,” *Phys. Rev. D* **85**, 055018 (2012), [arXiv:1108.4416 \[hep-ph\]](#).
- [20] M. Aoki, S. Kanemura, and K. Yagyu, “Testing the Higgs triplet model with the mass difference at the LHC,” *Phys. Rev. D* **85**, 055007 (2012), [arXiv:1110.4625 \[hep-ph\]](#).
- [21] A. G. Akeroyd and H. Sugiyama, “Production of doubly charged scalars from the decay of singly charged scalars in the Higgs Triplet Model,” *Phys. Rev. D* **84**, 035010 (2011), [arXiv:1105.2209 \[hep-ph\]](#).
- [22] C.-W. Chiang, T. Nomura, and K. Tsumura, “Search for doubly charged Higgs bosons using the same-sign diboson mode at the LHC,” *Phys. Rev. D* **85**, 095023 (2012), [arXiv:1202.2014 \[hep-ph\]](#).
- [23] A. G. Akeroyd, S. Moretti, and H. Sugiyama, “Five-lepton and six-lepton signatures from production of neutral triplet scalars in the Higgs Triplet Model,” *Phys. Rev. D* **85**, 055026 (2012), [arXiv:1201.5047 \[hep-ph\]](#).
- [24] E. J. Chun and P. Sharma, “Same-Sign Tetra-Leptons from Type II Seesaw,” *JHEP* **08**, 162 (2012), [arXiv:1206.6278 \[hep-ph\]](#).
- [25] F. del Aguila and M. Chala, “LHC bounds on Lepton Number Violation mediated by doubly and singly-charged scalars,” *JHEP* **03**, 027 (2014), [arXiv:1311.1510 \[hep-ph\]](#).
- [26] E. J. Chun and P. Sharma, “Search for a doubly-charged boson in four lepton final states in type II seesaw,” *Phys. Lett. B* **728**, 256–261 (2014), [arXiv:1309.6888 \[hep-ph\]](#).
- [27] S. Kanemura, K. Yagyu, and H. Yokoya, “First constraint on the mass of doubly-charged Higgs bosons in the same-sign diboson decay scenario at the LHC,” *Phys. Lett. B* **726**, 316–319 (2013), [arXiv:1305.2383 \[hep-ph\]](#).
- [28] S. Kanemura, M. Kikuchi, K. Yagyu, and H. Yokoya, “Bounds on the mass of doubly-charged Higgs bosons in the same-sign diboson decay scenario,” *Phys. Rev. D* **90**, 115018 (2014), [arXiv:1407.6547 \[hep-ph\]](#).
- [29] S. Kanemura, M. Kikuchi, H. Yokoya, and K. Yagyu, “LHC Run-I constraint on the mass of doubly charged Higgs bosons in the same-sign diboson decay scenario,” *PTEP* **2015**, 051B02 (2015), [arXiv:1412.7603 \[hep-ph\]](#).
- [30] Z. Kang, J. Li, T. Li, Y. Liu, and G.-Z. Ning, “Light Doubly Charged Higgs Boson via the  $WW^*$  Channel at LHC,” *Eur. Phys. J. C* **75**, 574 (2015), [arXiv:1404.5207 \[hep-ph\]](#).
- [31] Z.-L. Han, R. Ding, and Y. Liao, “LHC Phenomenology of Type II Seesaw: Nondegenerate Case,” *Phys. Rev. D* **91**, 093006 (2015), [arXiv:1502.05242 \[hep-ph\]](#).
- [32] Z.-L. Han, R. Ding, and Y. Liao, “LHC phenomenology of the type II seesaw mechanism: Observability of neutral scalars in the nondegenerate case,” *Phys. Rev. D* **92**, 033014 (2015), [arXiv:1506.08996 \[hep-ph\]](#).
- [33] M. Mitra, S. Niyogi, and M. Spannowsky, “Type-II Seesaw Model and Multilepton Signatures at Hadron Colliders,” *Phys. Rev. D* **95**, 035042 (2017), [arXiv:1611.09594 \[hep-ph\]](#).
- [34] D. K. Ghosh, N. Ghosh, I. Saha, and A. Shaw, “Revisiting the high-scale validity of the type II seesaw model with novel LHC signature,” *Phys. Rev. D* **97**, 115022 (2018), [arXiv:1711.06062 \[hep-ph\]](#).
- [35] S. Antusch, O. Fischer, A. Hammad, and C. Scherb, “Low scale type II seesaw: Present constraints and prospects for displaced vertex searches,” *JHEP* **02**, 157 (2019), [arXiv:1811.03476 \[hep-ph\]](#).
- [36] P. S. Bhupal Dev and Y. Zhang, “Displaced vertex signatures of doubly charged scalars in the type-II seesaw and its left-right extensions,” *JHEP* **10**, 199 (2018), [arXiv:1808.00943 \[hep-ph\]](#).
- [37] T. B. de Melo, F. S. Queiroz, and Y. Villamizar, “Doubly Charged Scalar at the High-Luminosity and High-Energy LHC,” *Int. J. Mod. Phys. A* **34**, 1950157 (2019), [arXiv:1909.07429 \[hep-ph\]](#).
- [38] R. Primulando, J. Julio, and P. Uttayarat, “Scalar phenomenology in type-II seesaw model,” *JHEP* **08**, 024 (2019), [arXiv:1903.02493 \[hep-ph\]](#).
- [39] E. J. Chun, S. Khan, S. Mandal, M. Mitra, and S. Shil, “Same-sign tetra-lepton signature at the Large Hadron Collider and a future  $pp$  collider,” *Phys. Rev. D* **101**, 075008 (2020), [arXiv:1911.00971 \[hep-ph\]](#).
- [40] R. Padhan, D. Das, M. Mitra, and A. Kumar Nayak, “Probing doubly and singly charged Higgs bosons at the  $pp$  collider HE-LHC,” *Phys. Rev. D* **101**, 075050 (2020), [arXiv:1909.10495 \[hep-ph\]](#).



- [41] S. Ashanujjaman and K. Ghosh, “Revisiting type-II see-saw: present limits and future prospects at LHC,” *JHEP* **03**, 195 (2022), [arXiv:2108.10952 \[hep-ph\]](#).
- [42] T. Nomura, H. Okada, and H. Yokoya, “Discriminating leptonic Yukawa interactions with doubly charged scalar at the ILC,” *Nucl. Phys. B* **929**, 193–206 (2018), [arXiv:1702.03396 \[hep-ph\]](#).
- [43] S. Blunier, G. Cottin, M. A. Díaz, and B. Koch, “Phenomenology of a Higgs triplet model at future  $e^+e^-$  colliders,” *Phys. Rev. D* **95**, 075038 (2017), [arXiv:1611.07896 \[hep-ph\]](#).
- [44] A. Crivellin, M. Ghezzi, L. Panizzi, G. M. Pruna, and A. Signer, “Low- and high-energy phenomenology of a doubly charged scalar,” *Phys. Rev. D* **99**, 035004 (2019), [arXiv:1807.10224 \[hep-ph\]](#).
- [45] P. Agrawal, M. Mitra, S. Niyogi, S. Shil, and M. Spannowsky, “Probing the Type-II Seesaw Mechanism through the Production of Higgs Bosons at a Lepton Collider,” *Phys. Rev. D* **98**, 015024 (2018), [arXiv:1803.00677 \[hep-ph\]](#).
- [46] L. Rahili, A. Arhrib, and R. Benbrik, “Associated production of SM Higgs with a photon in type-II seesaw models at the ILC,” *Eur. Phys. J. C* **79**, 940 (2019), [arXiv:1909.07793 \[hep-ph\]](#).
- [47] P. S. B. Dev, S. Khan, M. Mitra, and S. K. Rai, “Doubly-charged Higgs boson at a future electron-proton collider,” *Phys. Rev. D* **99**, 115015 (2019), [arXiv:1903.01431 \[hep-ph\]](#).
- [48] X.-H. Yang and Z.-J. Yang, “Doubly Charged Higgs Production at Future  $ep$  Colliders,” (2021), [arXiv:2103.11412 \[hep-ph\]](#).
- [49] F. F. Deppisch, P. S. Bhupal Dev, and A. Pilaftsis, “Neutrinos and Collider Physics,” *New J. Phys.* **17**, 075019 (2015), [arXiv:1502.06541 \[hep-ph\]](#).
- [50] Y. Cai, T. Han, T. Li, and R. Ruiz, “Lepton Number Violation: Seesaw Models and Their Collider Tests,” *Front. in Phys.* **6**, 40 (2018), [arXiv:1711.02180 \[hep-ph\]](#).
- [51] G. Aad *et al.* (ATLAS), “Search for doubly-charged Higgs bosons in like-sign dilepton final states at  $\sqrt{s} = 7$  TeV with the ATLAS detector,” *Eur. Phys. J. C* **72**, 2244 (2012), [arXiv:1210.5070 \[hep-ex\]](#).
- [52] S. Chatrchyan *et al.* (CMS), “A Search for a Doubly-Charged Higgs Boson in  $pp$  Collisions at  $\sqrt{s} = 7$  TeV,” *Eur. Phys. J. C* **72**, 2189 (2012), [arXiv:1207.2666 \[hep-ex\]](#).
- [53] G. Aad *et al.* (ATLAS), “Search for anomalous production of prompt same-sign lepton pairs and pair-produced doubly charged Higgs bosons with  $\sqrt{s} = 8$  TeV  $pp$  collisions using the ATLAS detector,” *JHEP* **03**, 041 (2015), [arXiv:1412.0237 \[hep-ex\]](#).
- [54] V. Khachatryan *et al.* (CMS), “Study of vector boson scattering and search for new physics in events with two same-sign leptons and two jets,” *Phys. Rev. Lett.* **114**, 051801 (2015), [arXiv:1410.6315 \[hep-ex\]](#).
- [55] “Search for a doubly-charged Higgs boson with  $\sqrt{s} = 8$  TeV  $pp$  collisions at the CMS experiment,” (2016).
- [56] “A search for doubly-charged Higgs boson production in three and four lepton final states at  $\sqrt{s} = 13$  TeV,” (2017).
- [57] M. Aaboud *et al.* (ATLAS), “Search for doubly charged Higgs boson production in multi-lepton final states with the ATLAS detector using proton–proton collisions at  $\sqrt{s} = 13$  TeV,” *Eur. Phys. J. C* **78**, 199 (2018), [arXiv:1710.09748 \[hep-ex\]](#).
- [58] A. M. Sirunyan *et al.* (CMS), “Observation of electroweak production of same-sign  $W$  boson pairs in the two jet and two same-sign lepton final state in proton-proton collisions at  $\sqrt{s} = 13$  TeV,” *Phys. Rev. Lett.* **120**, 081801 (2018), [arXiv:1709.05822 \[hep-ex\]](#).
- [59] M. Aaboud *et al.* (ATLAS), “Search for doubly charged scalar bosons decaying into same-sign  $W$  boson pairs with the ATLAS detector,” *Eur. Phys. J. C* **79**, 58 (2019), [arXiv:1808.01899 \[hep-ex\]](#).
- [60] G. Aad *et al.* (ATLAS), “Search for doubly and singly charged Higgs bosons decaying into vector bosons in multi-lepton final states with the ATLAS detector using proton-proton collisions at  $\sqrt{s} = 13$  TeV,” *JHEP* **06**, 146 (2021), [arXiv:2101.11961 \[hep-ex\]](#).
- [61] E. Accomando *et al.* (CLIC Physics Working Group), “Physics at the CLIC multi-TeV linear collider,” in *11th International Conference on Hadron Spectroscopy*, CERN Yellow Reports: Monographs (2004) [arXiv:hep-ph/0412251](#).
- [62] “The International Linear Collider Technical Design Report - Volume 2: Physics,” (2013), [arXiv:1306.6352 \[hep-ph\]](#).
- [63] A. Abada *et al.* (FCC), “FCC-ee: The Lepton Collider: Future Circular Collider Conceptual Design Report Volume 2,” *Eur. Phys. J. ST* **228**, 261–623 (2019).
- [64] M. Dong *et al.* (CEPC Study Group), “CEPC Conceptual Design Report: Volume 2 - Physics & Detector,” (2018), [arXiv:1811.10545 \[hep-ex\]](#).
- [65] A. Arhrib, R. Benbrik, M. Chabab, G. Moulhaka, M. C. Peyranere, L. Rahili, and J. Ramadan, “The Higgs Potential in the Type II Seesaw Model,” *Phys. Rev. D* **84**, 095005 (2011), [arXiv:1105.1925 \[hep-ph\]](#).
- [66] I. Esteban, M. C. Gonzalez-Garcia, M. Maltoni, T. Schwetz, and A. Zhou, “The fate of hints: updated global analysis of three-flavor neutrino oscillations,” *JHEP* **09**, 178 (2020), [arXiv:2007.14792 \[hep-ph\]](#).
- [67] P. A. Zyla *et al.* (Particle Data Group), “Review of Particle Physics,” *PTEP* **2020**, 083C01 (2020).
- [68] M. Aoki, S. Kanemura, M. Kikuchi, and K. Yagyu, “Radiative corrections to the Higgs boson couplings in the triplet model,” *Phys. Rev. D* **87**, 015012 (2013), [arXiv:1211.6029 \[hep-ph\]](#).
- [69] E. J. Chun, H. M. Lee, and P. Sharma, “Vacuum Stability, Perturbativity, EWPD and Higgs-to-diphoton rate in Type II Seesaw Models,” *JHEP* **11**, 106 (2012), [arXiv:1209.1303 \[hep-ph\]](#).
- [70] D. Das and A. Santamaria, “Updated scalar sector constraints in the Higgs triplet model,” *Phys. Rev. D* **94**, 015015 (2016), [arXiv:1604.08099 \[hep-ph\]](#).
- [71] A. M. Baldini *et al.* (MEG), “Search for the lepton flavour violating decay  $\mu^+ \rightarrow e^+\gamma$  with the full dataset of the MEG experiment,” *Eur. Phys. J. C* **76**, 434 (2016), [arXiv:1605.05081 \[hep-ex\]](#).
- [72] U. Bellgardt *et al.* (SINDRUM), “Search for the Decay  $\mu^+ \rightarrow e^+e^+e^-$ ,” *Nucl. Phys. B* **299**, 1–6 (1988).
- [73] M. Kakizaki, Y. Ogura, and F. Shima, “Lepton flavor violation in the triplet Higgs model,” *Phys. Lett. B* **566**, 210–216 (2003), [arXiv:hep-ph/0304254](#).
- [74] A. G. Akeroyd, M. Aoki, and H. Sugiyama, “Lepton Flavour Violating Decays  $\tau \rightarrow \bar{l}l$  and  $\mu \rightarrow e\gamma$  in the Higgs Triplet Model,” *Phys. Rev. D* **79**, 113010 (2009), [arXiv:0904.3640 \[hep-ph\]](#).
- [75] D. N. Dinh, A. Ibarra, E. Molinaro, and S. T. Petcov, “The  $\mu - e$  Conversion in Nuclei,  $\mu \rightarrow e\gamma$ ,  $\mu \rightarrow 3e$  Decays and TeV Scale See-Saw Scenarios of Neutrino Mass Generation,” *JHEP* **08**, 125 (2012), [Erratum: *JHEP* **09**, 023 (2013)], [arXiv:1205.4671 \[hep-ph\]](#).
- [76] F. Staub, “SARAH 4 : A tool for (not only SUSY) model builders,” *Comput. Phys. Commun.* **185**, 1773–1790 (2014), [arXiv:1309.7223 \[hep-ph\]](#).
- [77] F. Staub, “Exploring new models in all detail with SARAH,” *Adv. High Energy Phys.* **2015**, 840780 (2015), [arXiv:1503.04200 \[hep-ph\]](#).
- [78] C. Degrande, C. Duhr, B. Fuks, D. Grellscheid, O. Mattelaer, and T. Reiter, “UFO - The Universal FeynRules Output,” *Comput. Phys. Commun.* **183**, 1201–1214 (2012), [arXiv:1108.2040 \[hep-ph\]](#).
- [79] J. Alwall, M. Herquet, F. Maltoni, O. Mattelaer, and T. Stelzer, “MadGraph 5 : Going Beyond,” *JHEP* **06**, 128

- (2011), [arXiv:1106.0522 \[hep-ph\]](#).
- [80] J. Alwall, R. Frederix, S. Frixione, V. Hirschi, F. Maltoni, O. Mattelaer, H. S. Shao, T. Stelzer, P. Torrielli, and M. Zaro, “The automated computation of tree-level and next-to-leading order differential cross sections, and their matching to parton shower simulations,” *JHEP* **07**, 079 (2014), [arXiv:1405.0301 \[hep-ph\]](#).
- [81] T. Sjöstrand, S. Ask, J. R. Christiansen, R. Corke, N. Desai, P. Ilten, S. Mrenna, S. Prestel, C. O. Rasmussen, and P. Z. Skands, “An introduction to PYTHIA 8.2,” *Comput. Phys. Commun.* **191**, 159–177 (2015), [arXiv:1410.3012 \[hep-ph\]](#).
- [82] J. de Favereau, C. Delaere, P. Demin, A. Giammanco, V. Lemaître, A. Mertens, and M. Selvaggi (DELPHES 3), “DELPHES 3, A modular framework for fast simulation of a generic collider experiment,” *JHEP* **02**, 057 (2014), [arXiv:1307.6346 \[hep-ex\]](#).
- [83] M. Cacciari, G. P. Salam, and G. Soyez, “The anti- $k_t$  jet clustering algorithm,” *JHEP* **04**, 063 (2008), [arXiv:0802.1189 \[hep-ph\]](#).
- [84] M. Cacciari, G. P. Salam, and G. Soyez, “FastJet User Manual,” *Eur. Phys. J. C* **72**, 1896 (2012), [arXiv:1111.6097 \[hep-ph\]](#).
- [85] W. Verkerke and D. P. Kirkby, “The RooFit toolkit for data modeling,” eConf **C0303241**, MOLT007 (2003), [arXiv:physics/0306116](#).
- [86] R. Brun and F. Rademakers, “ROOT: An object oriented data analysis framework,” *Nucl. Instrum. Meth. A* **389**, 81–86 (1997).